Bimolecular reaction rates from ring polymer molecular dynamics: Application to H + CH4→ H2 + CH3

Yury V. Suleimanov, Rosana Collepardo-Guevara, and David E. Manolopoulos

Additional information on J. Chem. Phys.

Bimolecular reaction rates from ring polymer molecular dynamics: Application to H + CH$_4$ → H$_2$ + CH$_3$

Yury V. Suleimanov,[a] Rosana Collepardo-Guevara, and David E. Manolopoulos
Physical and Theoretical Chemistry Laboratory, University of Oxford, South Parks Road, Oxford OX1 3QZ, United Kingdom

In a recent paper, we have developed an efficient implementation of the ring polymer molecular dynamics (RPMD) method for calculating bimolecular chemical reaction rates in the gas phase, and illustrated it with applications to some benchmark atom–diatom reactions. In this paper, we show that the same methodology can readily be used to treat more complex polyatomic reactions in their full dimensionality, such as the hydrogen abstraction reaction from methane, H + CH$_4$ → H$_2$ + CH$_3$. The present calculations were carried out using a modified and recalibrated version of the Jordan–Gilbert potential energy surface. The thermal rate coefficients obtained between 200 and 2000 K are presented and compared with previous results for the same potential energy surface. Throughout the temperature range that is available for comparison, the RPMD approximation gives better agreement with accurate quantum mechanical (multiconfigurational time-dependent Hartree) calculations than do either the centroid density version of quantum transition state theory (QTST) or the quantum instanton (QI) model. The RPMD rate coefficients are within a factor of 2 of the exact quantum mechanical rate coefficients at temperatures in the deep tunneling regime. These results indicate that our previous assessment of the accuracy of the RPMD approximation for atom–diatom reactions remains valid for more complex polyatomic reactions. They also suggest that the sensitivity of the QTST and QI rate coefficients to the choice of the transition state dividing surface becomes more of an issue as the dimensionality of the reaction increases. © *2011 American Institute of Physics.* [doi:10.1063/1.3533275]

I. INTRODUCTION

The accurate and efficient calculation of chemical reaction rate coefficients is an important problem in computational chemistry. Classical molecular dynamics only provides reliable estimates of rate coefficients for reactions involving heavy atoms at high temperatures. At low temperatures, particularly for reactions involving the transfer of hydrogen atoms, quantum mechanical zero point energy and tunneling effects become critically important. The exact solution of the quantum reactive scattering Schrödinger equation is however still a very challenging task for systems containing more than a handful of atoms.[1] During last few decades, a number of approximate quantum mechanical methods have therefore been developed for calculating reaction rates that can be applied to more complex reactions in their full dimensionality.[2–18]

One of these approximate methods—the ring polymer molecular dynamics (RPMD) model developed in our research group[19,20]—is based on the isomorphism between the quantum statistical mechanics of the physical system and the classical statistical mechanics of a fictitious ring polymer consisting of *n* copies of the system connected by harmonic springs.[21] The resulting RPMD reaction rate theory[17,18] is essentially a classical rate theory in an extended (discretized imaginary time path integral) phase space, and this gives it some very desirable features. First, the RPMD rate becomes exact in the high temperature limit, where the ring polymer collapses to a single bead. It is also exact for a parabolic barrier bilinearly coupled to a bath of harmonic oscillators at all temperatures for which a rate coefficient can be defined.[17] Second, the theory has a well-defined short-time limit that provides an upper bound on the RPMD rate, in the same way as classical transition state theory provides an upper bound on the classical rate.[18] Indeed when the dividing surface is defined in terms of the centroid of the ring polymer the short-time limit of the RPMD rate coincides with a well-known (centroid density)[4–6] version of quantum transition state theory (QTST). Finally, and perhaps most importantly, the RPMD rate coefficient is rigorously independent of the choice of the transition state dividing surface that is used to compute it.[18] This is a highly desirable feature of the theory for applications to multidimensional reactions for which the optimum dividing surface can be very difficult to determine.

In our earlier papers, we have applied the RPMD theory to a number of simple model reactions, including one-dimensional symmetric and asymmetric barrier transmission problems[18] and a standard system-bath model for proton transfer in solution.[17] We have also applied it to some more complex problems, including a model for proton transfer from phenol to trimethylamine in liquid methyl chloride[22] and the intercavity hopping of hydrogen and muonium atoms in hexagonal ice.[23] Most recently, we have developed an efficient implementation of RPMD for bimolecular chemical reactions in the gas phase and applied it to the H + H$_2$, Cl + HCl, and F + H$_2$ reactions on *ab initio* electronic potential energy surfaces.[24]

[a]Electronic mail: yury.suleymanov@chem.ox.ac.uk.

134, 044131-1

Overall, the results of this earlier work have been quite encouraging. The RPMD approximation gives a reliable estimate of the rate coefficient in the high temperature regime of over-the-barrier dynamics, where it reproduces the exact quantum mechanical result in all cases where a comparison is available. As the temperature is lowered, the approximation increasingly overestimates the rates of asymmetric reactions and underestimates the rates of symmetric reactions.[18,24] Nevertheless, it correctly captures the dominant zero point energy and tunneling contributions to the rate coefficient even at very low temperatures, where it gives a rate that is usually within a factor of 2 of the exact quantum mechanical result.[18,24] Richardson and Althorpe[25] have recently explained these features of the approximation in their illuminating analysis of the connection between RPMD rate theory and the "Im F" version[26,27] of semiclassical instanton theory[28] in the deep quantum tunneling regime.

The methodology proposed in Ref. 24 for atom–diatom chemical reactions is based on the Bennett–Chandler approach.[29,30] A key feature of this methodology is that it does not require that one calculate the absolute value of either the reactant or the transition state partition function. Since the rate coefficient only depends on the ratio of these two partition functions it can be computed using well-established techniques such as umbrella sampling[31–34] or thermodynamic integration[33–37] along a suitable reaction coordinate. This procedure is rather universal and it can be extended in a straightforward way to treat more complex systems in their full dimensionality. Its application to polyatomic chemical reactions, for which accurate quantum results are now becoming available for comparison, is therefore desirable so as to validate the performance of the RPMD approximation for more complicated reactions than the atom–diatom reactions we have considered previously.[24]

The present study is a natural continuation of the work presented in Ref. 24. Here we apply the procedure developed there to the gas phase abstraction reaction between hydrogen and methane, $H + CH_4 \rightarrow H_2 + CH_3$. This is a prototypical atom–polyatomic reaction that is an important elementary step in hydrocarbon combustion chemistry.[38] In the past several years, it has been the subject of a variety of theoretical investigations. These include studies using various forms of classical transition state theory with tunneling corrections,[39–45] more elaborate QTST approaches,[46,47] reduced dimensionality quantum dynamical treatments,[48–54] and accurate quantum dynamics studies using the multiconfigurational time-dependent Hartree (MCTDH) method.[47,55–60] In this paper, we shall use the MCTDH rate coefficient to assess the accuracy of RPMD rate theory for the reaction and also compare this accuracy with that obtained from the quantum instanton (QI) model,[46] canonical variational transition state theory with a microcanonical tunneling (CVT/μOMT) correction,[43,47] and the centroid density version of QTST.

The paper is organized as follows. Section II summarizes the implementation of the RPMD method for polyatomic chemical reactions in the gas phase. Section III then presents the computational details of our calculations for the $H + CH_4$ reaction and compares the results of these calculations with those of earlier studies,[43,46,47] leaving Sec. IV to present our conclusions.

II. GENERAL METHODOLOGY

We shall first review the basics of the RPMD method and its application to gas phase chemical reactions, and then proceed to discuss the efficient numerical evaluation of RPMD thermal rate coefficients. For more detailed derivations of some of the working equations we refer the reader to Ref. 24. The only principally new aspect of the present methodology is the use of Cartesian atomic coordinates rather than the Jacobi coordinates that we used previously.[24] This is the standard approach in molecular dynamics simulations of complex systems, where introducing a new coordinate system that eliminates the center-of-mass motion is of negligible benefit compared with the ease of using Cartesian atomic coordinates.

A. Ring polymer molecular dynamics rate theory

Consider a general polyatomic chemical reaction involving N atoms in three-dimensional space with a Hamiltonian of the form

$$\hat{H} = \sum_{i=1}^{N} \frac{|\hat{\mathbf{p}}_i|^2}{2m_i} + V(\hat{\mathbf{r}}_1, \ldots, \hat{\mathbf{r}}_N), \tag{1}$$

where $\hat{\mathbf{p}}_i$ and $\hat{\mathbf{r}}_i$ are the momentum and position operators of atom i and m_i is its atomic mass.

As discussed in a number of recent papers,[17–20,22–24] RPMD is simply classical molecular dynamics in an extended (n-bead imaginary time path integral) phase space. The RPMD rate coefficient is thus[17,18,22,24]

$$k^{(n)}(T) = \frac{1}{Q_r^{(n)}(T)} \tilde{c}_{fs}^{(n)}(t \to \infty), \tag{2}$$

where $Q_r^{(n)}(T)$ is the n-bead path integral approximation to the quantum mechanical partition function of the reactants per unit volume and $\tilde{c}_{fs}^{(n)}(t)$ is a ring polymer flux-side correlation function,

$$\tilde{c}_{fs}^{(n)}(t) = \frac{1}{(2\pi\hbar)^{fn}} \int d^{fn}\mathbf{p}_0 \int d^{fn}\mathbf{r}_0 \, e^{-\beta_n H_n(\mathbf{p}_0, \mathbf{r}_0)}$$
$$\times \delta\left[s(\mathbf{r}_0)\right] v_s(\mathbf{p}_0, \mathbf{r}_0) h\left[s(\mathbf{r}_t)\right]. \tag{3}$$

Here $\beta_n = \beta/n$ with $\beta = 1/(k_B T)$ is the appropriate reciprocal temperature, $f = 3N$ is the total number of physical degrees of freedom, and $H_n(\mathbf{p}, \mathbf{r})$ is the Hamiltonian of a system of N three-dimensional n-bead harmonic ring polymers with an external potential of $V(\mathbf{r}_1, \ldots, \mathbf{r}_N)$ acting on each bead,

$$H_n(\mathbf{p}, \mathbf{r}) = H_n^0(\mathbf{p}, \mathbf{r}) + \sum_{j=1}^{n} V(\mathbf{r}_1^{(j)}, \ldots, \mathbf{r}_N^{(j)}), \tag{4}$$

where

$$H_n^0(\mathbf{p}, \mathbf{r}) = \sum_{i=1}^{N} \sum_{j=1}^{n} \left(\frac{|\mathbf{p}_i^{(j)}|^2}{2m_i} + \frac{1}{2} m_i \omega_n^2 |\mathbf{r}_i^{(j)} - \mathbf{r}_i^{(j-1)}|^2 \right), \tag{5}$$

with $\omega_n = 1/(\beta_n \hbar)$ and $\mathbf{r}_i^{(0)} \equiv \mathbf{r}_i^{(n)}$. Notice in particular that the mass of each bead j of the ith ring-polymer necklace has been set equal to the physical mass of the ith atom. This is the standard RPMD prescription,[19,20] which has recently been shown to be crucial for the accuracy of the resulting approximation to the quantum mechanical rate coefficient in the deep quantum tunneling regime.[25]

In Eq. (3), $s(\mathbf{r})$ is a reaction coordinate which becomes negative (positive) in the reactant (product) region, $v_s(\mathbf{p}_0, \mathbf{r}_0)$ is the velocity along this reaction coordinate

$$v_s(\mathbf{p}, \mathbf{r}) = \sum_{i=1}^{N} \sum_{j=1}^{n} \frac{\partial s(\mathbf{r})}{\partial \mathbf{r}_i^{(j)}} \cdot \frac{\mathbf{p}_i^{(j)}}{m_i} \tag{6}$$

at time $t = 0$, and $h[s(\mathbf{r}_t)]$ is a heaviside step function which counts ring polymer trajectories $(\mathbf{p}_t, \mathbf{r}_t)$ that are on the product side of the dividing surface at time t. Here the time-evolved coordinates $\mathbf{r}_t \equiv \mathbf{r}_t(\mathbf{p}_0, \mathbf{r}_0)$ and momenta $\mathbf{p}_t \equiv \mathbf{p}_t(\mathbf{p}_0, \mathbf{r}_0)$ are obtained from the classical dynamics generated by the ring polymer Hamiltonian $H_n(\mathbf{p}, \mathbf{r})$.[20]

Since none of the factors in the integrand of Eq. (3) depends on the location of center-of-mass of the ring polymer, the integral over the center-of-mass position diverges. However, this divergence is exactly cancelled by an identical divergence in $Q_r(T)$ in the expression for $k(T)$ in Eq. (2), and so it does not appear in any of the final working equations for the RPMD rate. The same issue arises in all other formulations of the rate problem that use Cartesian atomic coordinates without an explicit center-of-mass constraint. For example, the integrals in Eqs. (2.10) and (2.12) of Ref. 46 both diverge in the QI theory, but it is only the ratio of these two integrals that enters the expression for the QI rate.

The RPMD rate expression in Eq. (2) has the same structure as a classical rate theory,[61] and it reduces to a purely classical rate expression when the ring polymer is collapsed to a single bead ($n = 1$). As in the classical case, $\tilde{c}_{fs}^{(n)}(t)$ is a real and odd function of t which is discontinuous at $t = 0$ and has a positive limit as t tends to zero from above. This leads to a well-defined transition state theory approximation to the RPMD rate coefficient [18,22]

$$k_{\mathrm{QTST}}(s) = \frac{1}{Q_r^{(n)}(T)} \tilde{c}_{fs}^{(n)}(t \to 0_+; s), \tag{7}$$

where

$$\tilde{c}_{fs}^{(n)}(t \to 0_+; s) = \frac{1}{(2\pi\hbar)^{fn}} \int d^{fn}\mathbf{p}_0 \int d^{fn}\mathbf{r}_0 \, e^{-\beta_n H_n(\mathbf{p}_0, \mathbf{r}_0)}$$
$$\times \delta[s(\mathbf{r}_0)] \, v_s(\mathbf{p}_0, \mathbf{r}_0) h[v_s(\mathbf{p}_0, \mathbf{r}_0)]. \tag{8}$$

In writing these equations, we have explicitly indicated the dependence on s of $\tilde{c}_{fs}^{(n)}(t \to 0_+; s)$ and hence of $k_{\mathrm{QTST}}(s)$, which is a purely static equilibrium property that depends very strongly on the choice of the transition state dividing surface. In fact the dependence is exponential owing to the presence of $e^{-\beta_n H_n(\mathbf{p}_0, \mathbf{r}_0)} \delta[s(\mathbf{r}_0)]$ in the integrand of Eq. (8). On the other hand, the long-time limit of the flux-side correlation function $\tilde{c}_{fs}^{(n)}(t \to \infty)$, and hence the RPMD rate coefficient $k^{(n)}(T)$ in Eq. (2), is a dynamical property that is entirely

independent of the choice of the dividing surface.[18] $k^{(n)}(T)$ is related to $k_{\mathrm{QTST}}(s)$ through the transmission coefficient

$$\kappa^{(n)}(s) = \frac{k^{(n)}(T)}{k_{\mathrm{QTST}}(s)} = \frac{\tilde{c}_{fs}^{(n)}(t \to \infty)}{\tilde{c}_{fs}^{(n)}(t \to 0_+; s)}, \tag{9}$$

which contains a dynamical correction to the transition state theory approximation to the rate.

The dividing surface $s(\mathbf{r}) = 0$ is usually defined in terms of the ring polymer centroid variables[18]

$$s(\bar{\mathbf{r}}) \equiv s(\bar{\mathbf{r}}_1, \ldots, \bar{\mathbf{r}}_N), \tag{10}$$

where

$$\bar{\mathbf{r}}_i = \frac{1}{n} \sum_{j=1}^{n} \mathbf{r}_i^{(j)}. \tag{11}$$

In this case, $k_{\mathrm{QTST}}(s)$ coincides with the rate coefficient given by the well-known centroid-density version of QTST.[4–6,18] Richardson and Althorpe[25] have recently explained why a dividing surface based on centroid variables is the optimum choice at temperatures above the crossover temperature $T_c = \hbar\omega_b/2\pi k_B$, where $i\omega_b$ is the imaginary frequency at the top of the reaction barrier. The excited modes of the ring polymer begin to contribute to the optimum dividing surface in the "deep tunneling" regime below this crossover temperature.[25] One can however still continue to use a dividing surface based on centroid variables at temperatures below T_c in the RPMD theory, as the transmission coefficient $\kappa^{(n)}(s)$ will correct for any deficiencies in this choice and give exactly the same rate coefficient as one would have obtained using any other dividing surface.[18,25]

B. Bennett–Chandler factorization

To proceed to an efficient numerical procedure for evaluating the RPMD rate coefficient, we noted in Ref. 24 that the expression for $k_{\mathrm{QTST}}(s)$ in Eq. (7) simplifies dramatically when one uses a dividing surface located in the asymptotic reactant valley. The definition of this dividing surface is[24,46,62]

$$s_0(\bar{\mathbf{r}}) = R_\infty - \left| \bar{\mathbf{R}} \right| = 0, \tag{12}$$

where $\bar{\mathbf{R}}$ is the centroid of the vector that connects the centers of mass of the reactant molecules A and B,

$$\bar{\mathbf{R}} = \frac{1}{m_B} \sum_{i \in B} m_i \bar{\mathbf{r}}_i - \frac{1}{m_A} \sum_{i \in A} m_i \bar{\mathbf{r}}_i, \tag{13}$$

and R_∞ is an adjustable parameter that is chosen to be sufficiently large as to make the interaction between the reactants negligible. The QTST rate coefficient for this dividing surface is simply[24]

$$k_{\mathrm{QTST}}(s_0) = 4\pi R_\infty^2 \left(\frac{1}{2\pi\beta\mu_R} \right)^{1/2}, \tag{14}$$

where

$$\mu_R = \frac{m_A m_B}{m_A + m_B}. \tag{15}$$

In other words, $k_{QTST}(s_0)$ is just the surface area of a sphere with radius R_∞ times the thermally averaged flux of reactants entering this sphere.[24]

The dynamical correction $\kappa^{(n)}(s)$ to the QTST rate will however be very small for this dividing surface, owing to the presence of the factors of $e^{-\beta_n H_n(\mathbf{p}_0, \mathbf{r}_0)} \delta[s(\mathbf{r}_0)]$ in Eqs. (3) and (8). This suggests introducing a second dividing surface $s_1(\bar{\mathbf{r}}) = 0$ located in the transition state region and writing the corresponding transition theory rate coefficient as

$$k_{QTST}(s_1) = p^{(n)}(s_1, s_0) k_{QTST}(s_0), \tag{16}$$

in which the first factor is a ratio of ring polymer flux-side correlation functions for two different dividing surfaces in the limit as $t \to 0_+$,

$$p^{(n)}(s_1, s_0) = \frac{\tilde{c}_{fs}^{(n)}(t \to 0_+; s_1)}{\tilde{c}_{fs}^{(n)}(t \to 0_+; s_0)}. \tag{17}$$

Combining this with the transmission coefficient $\kappa^{(n)}(s_1)$ for the dividing surface $s_1(\bar{\mathbf{r}}) = 0$ yields the following expression for the RPMD rate coefficient $k^{(n)}(T)$,[24]

$$
\begin{aligned}
k^{(n)}(T) &= \kappa^{(n)}(s_1) k_{QTST}(s_1) \\
&= \kappa^{(n)}(s_1) p^{(n)}(s_1, s_0) k_{QTST}(s_0),
\end{aligned} \tag{18}
$$

where $k_{QTST}(s_0)$ is given analytically in Eq. (14).

With this (Bennett–Chandler)[29,30] factorization, the rate calculation has been split into two separate stages: the evaluation of the transmission coefficient $\kappa^{(n)}(s_1)$ for a dividing surface located in the transition state region and the evaluation of the corresponding transition state theory rate coefficient $k_{QTST}(s_1)$. A notable feature of the latter of these two calculations is the use of two separate dividing surfaces, one located near the transition state $[s_1(\bar{\mathbf{r}}) = 0]$ and the other in the reactant asymptote $[s_0(\bar{\mathbf{r}}) = 0]$. As we shall describe in more detail in the following section, $p^{(n)}(s_1, s_0)$ in Eq. (17) can be efficiently calculated from the reversible work done in taking a system with a modified ring polymer Hamiltonian from one of these dividing surfaces to the other. Another important observation from Eq. (18) is that, with this computational strategy, one does not need to calculate the absolute value of the reactant partition function $Q_r(T)$. This is particularly convenient in the case of polyatomic reactions, for which $Q_r(T)$ can be difficult to calculate exactly.[47,63–65] Note also that the same strategy can be used to calculate purely classical reaction rates simply by replacing the ring polymer with a single bead ($n = 1$).

C. Computational strategy

We shall now summarize all of the working equations that are needed to evaluate the RPMD rate coefficient using Eq. (18). We first focus on $p^{(n)}(s_1, s_0)$, which determines the centroid density QTST rate coefficient. According to Eq. (17), $p^{(n)}(s_1, s_0)$ is the ratio of two static equilibrium quantities, one associated with the top of the potential energy barrier and the other with the reactant asymptote. After some manipulations described in Ref. 24, it can be rewritten as

$$p^{(n)}(s_1, s_0) = P^{(n)}(1)/P^{(n)}(0), \tag{19}$$

where

$$P^{(n)}(\xi) = \frac{\int d^{fn}\mathbf{p} \int d^{fn}\mathbf{r}\, e^{-\beta_n H_n^s(\mathbf{p}, \mathbf{r})} \delta[s(\bar{\mathbf{r}}) - \xi]}{\int d^{fn}\mathbf{p} \int d^{fn}\mathbf{r}\, e^{-\beta_n H_n^s(\mathbf{p}, \mathbf{r})}} \tag{20}$$

is the probability that an interpolating reaction coordinate $s(\bar{\mathbf{r}})$ takes the value ξ in the equilibrium canonical ensemble of a system with the following modified ring polymer Hamiltonian

$$H_n^s(\mathbf{p}, \mathbf{r}) = H_n(\mathbf{p}, \mathbf{r}) - \frac{1}{\beta_n} \ln f_s(\bar{\mathbf{r}}), \tag{21}$$

where

$$f_s(\bar{\mathbf{r}}) = \left\{ \sum_{i=1}^{N} \frac{1}{2\pi\beta m_i} \left| \frac{\partial s(\bar{\mathbf{r}})}{\partial \bar{\mathbf{r}}_i} \right|^2 \right\}^{1/2}. \tag{22}$$

A suitable interpolating reaction coordinate $s(\bar{\mathbf{r}})$ that connects two dividing surfaces was originally proposed by Yamamoto and Miller in a closely related context and is given by[46,62]

$$s(\bar{\mathbf{r}}) = \frac{s_0(\bar{\mathbf{r}})}{s_0(\bar{\mathbf{r}}) - s_1(\bar{\mathbf{r}})}. \tag{23}$$

Note that, with this definition, $s(\bar{\mathbf{r}}) \to 0$ as $s_0(\bar{\mathbf{r}}) \to 0$ and $s(\bar{\mathbf{r}}) \to 1$ as $s_1(\bar{\mathbf{r}}) \to 0$. In particular, the transition state dividing surface $s_1(\bar{\mathbf{r}}) = 0$ in the region of the reaction barrier now occurs at $s(\bar{\mathbf{r}}) = 1$.

It follows from Eq. (19) that $p^{(n)}(s_1, s_0)$ can be expressed as

$$p^{(n)}(s_1, s_0) = e^{-\beta[W(1) - W(0)]}, \tag{24}$$

where $W(\xi)$ is the centroid potential of mean force (or free energy) associated with the probability distribution $P^{(n)}(\xi)$,

$$W(\xi) = -\frac{1}{\beta} \ln P^{(n)}(\xi). \tag{25}$$

Various methods can be employed to calculate the free energy difference $W(1) - W(0)$ in Eq. (24). When the reaction barrier is significantly higher than the available thermal energy $k_B T$, the problem of poor sampling in the barrier region is usually overcome by performing biased (umbrella sampling)[31–34] or constrained (thermodynamic integration)[33–37] molecular dynamics simulations. In the present work, we have used the umbrella integration method of Kästner and Thiel,[66–68] which is closely related to both of these techniques.[67]

In umbrella integration, the reaction coordinate is divided into a series of windows and a harmonic umbrella potential

$$w_i(\bar{\mathbf{r}}) = \tfrac{1}{2} k(s(\bar{\mathbf{r}}) - \xi_i)^2 \tag{26}$$

is placed in each window i. Here the force constant k defines the strength of the bias. The biased mean forces $\partial W_i(\xi)/\partial \xi$ are calculated for each window using the local probability distributions $P_i^{(n)}(\xi)$ and then corrected for the effect of the bias to yield a global solution to the unbiased mean force $\partial W(\xi)/\partial \xi$ on a grid in ξ. The free energy difference $W(1) - W(0)$ is then calculated by integrating $\partial W(\xi)/\partial \xi$ numerically along ξ.[66,67]

The potential of mean force $W(\xi)$ exhibits a barrierlike profile that is strongly related to the underlying potential energy surface. For an asymmetric reaction, the location of the

barrier maximum $\xi^\ddagger$ can deviate from one, as was seen in our previous study of the F + H$_2$ reaction.[24] Although the full RPMD rate coefficient is independent of the choice of dividing surface, it is sensible to choose it to be at the top of the free energy barrier so as to minimize the centroid density QTST rate and reduce the recrossing of the dividing surface in the subsequent calculation of the transmission coefficient. Such a variational optimization increases the ring polymer transmission coefficient by the same factor as it decreases the centroid density QTST rate. For asymmetric reactions, it is therefore computationally advantageous to replace Eq. (18) by

$$k^{(n)}(T) = \kappa^{(n)}(s_\ddagger) k_{\mathrm{QTST}}(s_\ddagger) = \kappa^{(n)}(s_\ddagger) p^{(n)}(s_\ddagger, s_0) k_{\mathrm{QTST}}(s_0),$$
(27)

where the transmission coefficient $\kappa^{(n)}(s_\ddagger)$ is now calculated for $s(\bar{\mathbf{r}}) = \xi^\ddagger$ and

$$p^{(n)}(s_\ddagger, s_0) = e^{-\beta[W(\xi^\ddagger) - W(0)]}.$$
(28)

The treatment of the remaining factor $\kappa^{(n)}(s_\ddagger)$ is rather straightforward. Combining Eqs. (3), (8), and (9) gives

$$\kappa^{(n)}(s_\ddagger) = \lim_{t \to \infty} \frac{\langle v_s(\mathbf{p}_0, \mathbf{r}_0) h[s(\bar{\mathbf{r}}_t) - \xi^\ddagger] \delta[s(\bar{\mathbf{r}}_0) - \xi^\ddagger] \rangle}{\langle v_s(\mathbf{p}_0, \mathbf{r}_0) h[v_s(\bar{\mathbf{p}}_0, \bar{\mathbf{r}}_0)] \delta[s(\bar{\mathbf{r}}_0) - \xi^\ddagger] \rangle},$$
(29)

where the angular brackets denote a canonical average

$$\langle \cdots \rangle = \frac{\int d^{fn}\mathbf{p}_0 \int d^{fn}\mathbf{r}_0 e^{-\beta_n H_n(\mathbf{p}_0, \mathbf{r}_0)} (\cdots)}{\int d^{fn}\mathbf{p}_0 \int d^{fn}\mathbf{r}_0 e^{-\beta_n H_n(\mathbf{p}_0, \mathbf{r}_0)}},$$
(30)

and the presence of the delta function $\delta[s(\bar{\mathbf{r}}_0) - \xi^\ddagger]$ in the numerator and denominator of Eq. (29) implies that the average can be taken over a constrained distribution in which the centroid of the ring polymer is on the dividing surface. For actual molecular dynamics simulations with the hard constraint $s(\bar{\mathbf{r}}_0) = \xi^\ddagger$, the appropriate form of Eq. (29) is[24]

$$\kappa^{(n)}(s_\ddagger) = \lim_{t \to \infty} \frac{\left\langle f_s(\bar{\mathbf{r}}_0)^{-1} v_s(\mathbf{p}_0, \mathbf{r}_0) h[s(\bar{\mathbf{r}}_t) - \xi^\ddagger] \right\rangle_s}{\left\langle f_s(\bar{\mathbf{r}}_0)^{-1} v_s(\mathbf{p}_0, \mathbf{r}_0) h[v_s(\bar{\mathbf{p}}_0, \bar{\mathbf{r}}_0)] \right\rangle_s},$$
(31)

where the subscripts on the brackets indicate that the averages are now over the constrained ensemble and the factor of $f_s(\bar{\mathbf{r}}_0)^{-1}$ is a metric tensor correction for the effect of the constraint.[24,33]
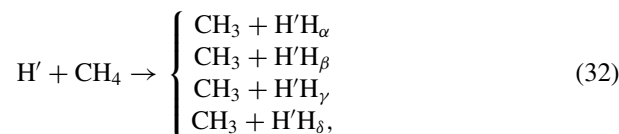
The transmission coefficient can be evaluated from Eq. (31) by performing a constrained RPMD simulation in the presence of a thermostat to obtain an average of the bracketed quantity in the denominator and generate a series of independent configurations $\mathbf{r}_0$ with centroids on the transition state dividing surface $s(\bar{\mathbf{r}}_0) = \xi^\ddagger$. For each of these configurations, we then sample a number of momentum vectors $\mathbf{p}_0$ at random from the Maxwell distribution contained in $e^{-\beta_n H_n(\mathbf{p}_0, \mathbf{r}_0)}$ and evolve the resulting trajectories forwards in time (without the thermostat or the dividing surface constraint) to obtain $\mathbf{r}_t$. The bracketed quantity in the numerator is calculated by averaging over a large number of these trajectories. Note that Eq. (31) differs slightly from the (formally equivalent) expression we used to compute the transmission coefficient for atom–diatom reactions in Eq. (65) of Ref. 24. We have since found that it is more convenient to use Eq. (31) as it provides slightly better convergence and ensures that the

time-dependent transmission coefficient tends exactly to one as $t \to 0_+$.

III. APPLICATION TO H + CH$_4$

A. Computational details

We now apply the above computational strategy to the reaction of a hydrogen atom with a methane molecule and discuss some specific details of the numerical calculations. This reaction has four product arrangement channels

$$\text{H}' + \text{CH}_4 \rightarrow \begin{cases} \text{CH}_3 + \text{H}'\text{H}_\alpha \\ \text{CH}_3 + \text{H}'\text{H}_\beta \\ \text{CH}_3 + \text{H}'\text{H}_\gamma \\ \text{CH}_3 + \text{H}'\text{H}_\delta, \end{cases}$$
(32)

all of which contribute equally to the reaction rate. Following Zhao *et al.*,[46] we can take this into account by specifying the dividing surface $s_1(\bar{\mathbf{r}}) = 0$ in the region of the reaction barrier as

$$s_1(\bar{\mathbf{r}}) = \max\left\{ s_{1\alpha}(\bar{\mathbf{r}}), s_{1\beta}(\bar{\mathbf{r}}), s_{1\gamma}(\bar{\mathbf{r}}), s_{1\delta}(\bar{\mathbf{r}}) \right\},$$
(33)

where $s_{1x}(\bar{\mathbf{r}}) = 0$ is the dividing surface associated with one of the individual channels in Eq. (32),

$$s_{1x}(\bar{\mathbf{r}}) = (|\bar{\mathbf{r}}_{\text{CH}_x}| - r^\ddagger_{\text{CH}_x}) - (|\bar{\mathbf{r}}_{\text{H}'\text{H}_x}| - r^\ddagger_{\text{H}'\text{H}_x}).$$
(34)

Here $\bar{\mathbf{r}}_{\text{AB}}$ denotes the vector that connects the centroids of atoms A and B and $r^\ddagger_{\text{AB}}$ is the corresponding interatomic distance at the transition state saddle point. Clearly, with the definition in Eq. (33), all four product channels are treated equivalently.[46]

The computational details of the present RPMD simulations were as follows. All calculations were performed using Cartesian atomic coordinates with the ring polymer Hamiltonian in Eqs. (4) and (5), thus imposing no restriction on the overall rotational or translational motion of the $N = 6$ atom system. We chose to employ a modified and recalibrated version of the Jordan–Gilbert[69] potential energy surface developed by Espinosa-García (PJEG).[43] It should be noted that this is a rather old semi-empirical potential which is known to have serious deficiencies.[45,70] For example, the reaction barrier height and the imaginary frequency at the saddle point are significantly lower than recent *ab initio* calculations indicate.[58,59,71,72] As a result, one would not expect the rate coefficients calculated using PJEG to agree well with those calculated using newer potentials[59,71,72] or with experiment.[73,74] However, reaction rates have been obtained for this potential using the QI model[46] and a number of other approximate methods,[43,47] and accurate quantum mechanical results are available for comparison from the MCTDH method.[47] It is therefore an appropriate choice of potential for our present purpose, which is simply to compare the accuracy of the RPMD approximation with that of these other approaches.

The thermal rate coefficients were calculated at 11 temperatures ranging from 200 to 2000 K in steps of 100 K for $T \leq 1000$ K and 500 K for $1000 \leq T \leq 2000$ K. Additional calculations were performed at 225 K for the purpose of comparison with the MCTDH results (see Table II below).

TABLE I. Various quantities obtained for the H + CH$_4 \rightarrow$ H$_2$ + CH$_3$ reaction in the present calculations. $\xi_{cl}^\ddagger$ and $\xi_{RPMD}^\ddagger$ are the positions of the maxima along the reaction coordinate ξ in the classical and centroid potentials of mean force, respectively. $k_{TST}(s_\ddagger)$ and $k_{QTST}(s_\ddagger)$ are the corresponding classical and centroid density quantum transition state theory rate coefficients, and $\kappa_{cl}(s_\ddagger)$ and $\kappa_{RPMD}(s_\ddagger)$ are the classical and RPMD transmission coefficients. The TST and QTST rates are given in cm^3 molecule^{-1} s^{-1} and the numbers in parentheses denote powers of 10.

	Classical			RPMD		
T / K	$\xi_{cl}^\ddagger$	$\kappa_{cl}(s_\ddagger)$	$k_{TST}(s_\ddagger)$	$\xi_{RPMD}^\ddagger$	$\kappa_{RPMD}(s_\ddagger)$	$k_{QTST}(s_\ddagger)$
200	1.019	0.903	1.24(−25)	1.030	0.652	2.50(−22)
225	1.019	0.901	5.37(−24)	1.029	0.676	2.87(−21)
300	1.018	0.893	8.08(−21)	1.026	0.723	6.54(−19)
400	1.018	0.891	3.59(−18)	1.024	0.738	5.26(−17)
500	1.018	0.884	1.25(−16)	1.022	0.752	8.66(−16)
600	1.017	0.881	1.42(−15)	1.020	0.768	5.99(−15)
700	1.017	0.878	8.10(−15)	1.019	0.784	2.59(−14)
800	1.017	0.874	3.15(−14)	1.018	0.796	7.89(−14)
900	1.016	0.870	9.04(−14)	1.018	0.805	1.96(−13)
1000	1.016	0.869	2.14(−13)	1.017	0.811	4.08(−13)
1500	1.015	0.856	3.33(−12)	1.015	0.826	4.50(−12)
2000	1.013	0.851	1.51(−11)	1.013	0.830	1.80(−11)

One hundred twenty eight ring polymer beads were used for $T \leq 300$ K, 64 beads for $400 \leq T \leq 600$ K, and 32 beads for $700 \leq T \leq 2000$ K. The parameter R_∞ in Eq. (12) was set to 30 bohr for all of the temperatures considered.

The centroid density QTST rate coefficients $k_{QTST}(s_\ddagger)$ were calculated using umbrella integration as described in Sec. II C. One hundred twenty one biasing windows were spaced evenly in the interval $-0.05 \leq \xi \leq 1.15$. After some preliminary tests, the force constant k in Eq. (26) was chosen to be 2.72 (nT/K) eV for all windows (the same as the value we used for atom–diatom reactions in Ref. 24). In each umbrella window i, the system was equilibrated for 20 ps and

TABLE II. Comparison of theoretical rate coefficients for the H + CH$_4 \rightarrow$ H$_2$ + CH$_3$ reaction on the PJEG potential energy surface (Ref. 43). k_{QI} is the quantum instanton rate coefficient from Ref. 46. $k_{CVT/\mu OMT}$ is the canonical variational transition state theory/microcanonical optimized multidimensional tunneling rate coefficient from Refs. 47 (for $T \leq 400$ K) and 43 (for $T \geq 500$ K). k_{MCTDH} is the multiconfigurational time-dependent Hartree rate coefficient from Ref. 47. k_{cl} and k_{RPMD} are the classical and RPMD rate coefficients obtained from the data in Table I. All the rates are given in cm^3 molecule^{-1} s^{-1} and numbers in parentheses denote powers of 10.

T / K	k_{QI}	$k_{CVT/\mu OMT}$	k_{RPMD}	k_{MCTDH}	k_{cl}
200	3.30(−22)	1.87(−22)	1.63(−22)	—	1.12(−25)
225	—	2.28(−21)	1.94(−21)	1.01(−21)	4.84(−24)
300	7.80(−19)	5.06(−19)	4.73(−19)	2.81(−19)	7.21(−21)
400	6.00(−17)	4.17(−17)	3.93(−17)	2.81(−17)	3.19(−18)
500	9.00(−16)	6.96(−16)	6.51(−16)	—	1.11(−16)
600	5.42(−15)	5.00(−15)	4.60(−15)	—	1.25(−15)
700	2.40(−14)	—	2.03(−14)	—	7.11(−15)
800	7.13(−14)	6.72(−14)	6.28(−14)	—	2.75(−14)
900	1.85(−13)	—	1.58(−13)	—	7.87(−14)
1000	3.97(−13)	3.58(−13)	3.31(−13)	—	1.86(−13)
1500	—	4.20(−12)	3.72(−12)	—	2.85(−12)
2000	1.52(−11)	1.70(−11)	1.49(−11)	—	1.29(−11)

the local biased distribution functions $P_i^{(n)}(\xi)$ were then accumulated along a 10 ns trajectory in the presence of an Andersen thermostat.[75] The ring polymer equations of motion were integrated using a symplectic algorithm involving alternating free ring polymer evolutions and momentum updates,[76] with a time step of 0.1 fs.

Having obtained the optimal values of $\xi^\ddagger$ for each temperature, we calculated the transmission coefficients $\kappa^{(n)}(s_\ddagger)$ as described at the end of Sec. II C. The RATTLE[77] algorithm was introduced into the time integration to constrain the centroid $\bar{\mathbf{r}}$ to the dividing surface $s(\bar{\mathbf{r}}) = \xi^\ddagger$. The simulations were initiated by running a long (20 ns) mother trajectory along which, after an initial equilibration period of 20 ps, constrained configurations were sampled once every 2 ps. For each of these configurations, we then ran 50 separate unconstrained trajectories for 0.1 ps with different initial momenta to accumulate the transmission coefficient. Both the constrained and the unconstrained simulations were performed with a time step of 0.1 fs, but with the thermostat switched off for the latter.

The parameters used in these two procedures were checked to be sufficient to converge both $k_{QTST}(s_\ddagger)$ and $\kappa^{(n)}(s_\ddagger)$ to within a statistical error of 1%–2%. We also performed classical simulations in which the ring polymer was replaced with a single bead ($n = 1$), using entirely analogous procedures to calculate the classical TST rate coefficient and the classical transmission coefficient.

B. Transition state theory rates and transmission coefficients

The results of the above RPMD and classical simulations are summarized in Table I. The potential of mean force along the reaction coordinate ξ and the time-dependent transmission coefficients obtained at two representative temperatures (200 and 1000 K) are also plotted in Figs. 1 and 2, respectively, to focus our discussion of these simulations.

Figure 1 shows that the free energy profiles obtained from the classical and RPMD simulations differ quite noticeably, especially at the lower of the two temperatures. According to Table I, the centroid density QTST rate is larger than the classical TST rate by a factor of 2 at 1000 K and by more than 3 orders of magnitude at 200 K. This quantum mechanical enhancement of the rate at low temperatures is of course to be expected since the reaction involves the tunneling of a hydrogen atom.

Notice also from Fig. 1 that the maxima in the classical and centroid free energy barriers occur for values of ξ greater than one. This is best seen at 200 K, where the maxima in the classical ($\xi_{cl}^\ddagger$) and centroid ($\xi_{RPMD}^\ddagger$) free energy curves are located at 1.019 and 1.030, respectively. Table I shows that $\xi_{cl}^\ddagger$ and $\xi_{RPMD}^\ddagger$ both decrease as the temperature increases, the two values approaching each other and nearly coinciding for $T \geq 1500$ K. However, the maxima are not exactly at $\xi = 1$ even at the highest temperature we have considered ($T = 2000$ K). Clearly, the dividing surface $s(\bar{\mathbf{r}}) = 1$ is less than optimal for this reaction, and the variational flexibility afforded by displacing $\xi^\ddagger$ from one to improve the dividing
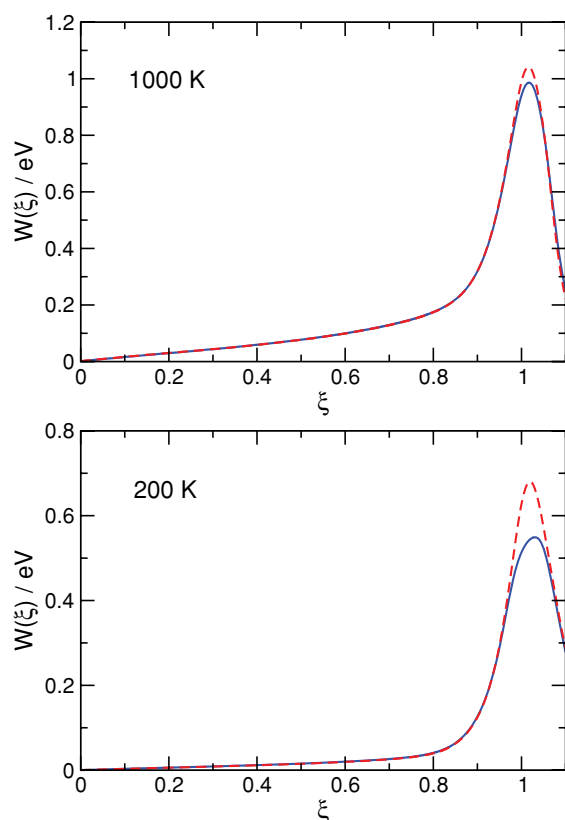
FIG. 1. Classical (dashed red) and centroid (solid blue) potentials of mean force for the H + CH$_4$ reaction at 1000 and 200 K.

FIG. 2. Classical (dashed red) and RPMD (solid blue) time-dependent transmission coefficients for the H + CH$_4$ reaction at 1000 and 200 K.

surface is therefore useful. At $T = 200$ K, for instance, the centroid density QTST rate evaluated at $\xi = \xi^{\ddagger}$ is smaller than that obtained at $\xi = 1$ by a factor of ~ 8, and in the classical limit the optimization reduces the TST rate by a factor of ~ 22. However, it is clear that even if we choose the optimum value of $\xi^{\ddagger}$ at each temperature, the recrossing of the dividing surface will not be suppressed completely, because the functional form we have used for $s_1(\bar{\mathbf{r}})$ in Eq. (33) [and hence $s(\bar{\mathbf{r}})$ in Eq. (23)] is itself unlikely to be optimal for a reaction with this many degrees of freedom.

Figure 2 shows that some of the classical and ring polymer trajectories do indeed recross the variationally optimum dividing surface at $\xi = \xi^{\ddagger}$, particularly in the ring polymer case. In both cases, the time-dependent transmission coefficients decay rapidly from one and reach plateau values rather quickly (within 50 fs). The converged classical transmission coefficient $\kappa_{\mathrm{cl}}(s_{\ddagger})$ is around 0.87 at 1000 K and 0.90 at 200 K and therefore increases slightly with decreasing temperature. This temperature dependence in the classical simulations is as expected—the lower available thermal energy at lower temperatures should lead to less recrossing of a suitably chosen dividing surface.

The RPMD results in Fig. 2 require more explanation. The converged ring polymer transmission coefficient $\kappa_{\mathrm{RPMD}}(s_{\ddagger})$ is generally smaller than the classical transmission coefficient and it exhibits the opposite temperature dependence. It is around 0.81 at 1000 K and 0.65 at 200 K. The smaller values of $\kappa_{\mathrm{RPMD}}(s_{\ddagger})$ at lower temperatures imply that the dividing surface becomes less than optimum in the RPMD
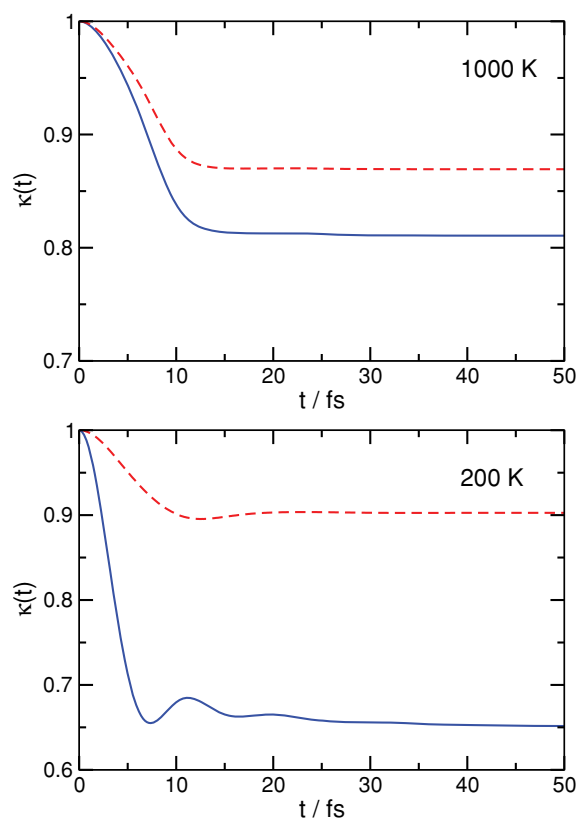
case as the temperature decreases. The most likely reason for this is that the dividing surface $s_1(\bar{\mathbf{r}}) = 0$ in Eqs. (33) and (34) is constrained to be a function of the ring polymer centroid variables. In their recent study of one-dimensional barrier transition problems, Richardson and Althorpe[25] have shown that the other normal modes of the ring polymer start to contribute to the optimum reaction coordinate in the deep tunneling regime below the crossover temperature $T_c = \hbar\omega_b/2\pi k_{\mathrm{B}}$, which is 296 K for the present reaction. We therefore believe that the centroid expression for the dividing surface is the reason for the enhanced transition state recrossing in the present RPMD simulations at low temperatures. A similar temperature dependence of the RPMD transmission coefficients was observed in our previous study of atom–diatom reactions,[24] in which we also used a dividing surface based on centroid variables.

The recrossing of the centroid dividing surface is expected to be particularly severe for reactions with asymmetric barriers, for which the first two (degenerate) excited normal modes of the ring polymer begin to contribute significantly to the optimum reaction coordinate as soon as the temperature is lowered through T_c.[25] This is the reason for the well-known deficiency of centroid density QTST for asymmetric reactions in the deep quantum tunneling regime.[25,78,79] In our recent study of the F + H$_2$ reaction,[24] centroid density QTST was found to provide a rate coefficient that actually increased on decreasing the temperature from 300 to 200 K, an unphysical effect that has also been seen previously in a study of a one-dimensional asymmetric barrier transmission problem.[27]

However, one sees from Table I that the QTST rate coefficient for the H + CH₄ reaction decreases monotonically with decreasing temperature down to the lowest temperature we have considered ($T = 200$ K). It is possible that an unphysical increase would eventually be observed in the QTST rate if the temperature were lowered even further, but we have not performed these calculations as they require a larger number of ring polymer beads. In any event, the RPMD theory is immune to this problem as its transmission coefficient corrects for the use of a centroid-based dividing surface and gives the same rate as would have been obtained using any other dividing surface, even in the deep tunneling regime.[25]

C. Comparison with earlier work

The rate coefficients we actually obtain for the H + CH₄ reaction by combining the QTST rates with the RPMD transmission coefficients are presented along with the corresponding classical results in Table II. This table also includes the results obtained by Andersson *et al.*[47] using the MCTDH method, the results obtained by Andersson *et al.*[47] and Espinosa-García[43] using the CVT/μOMT approximation, and the results obtained by Zhao *et al.*[46] using the QI model. All the calculations were performed using the PJEG potential energy surface.[43] Andersson *et al.* also reported some results obtained using harmonic transition state theory (HTST) and harmonic quantum transition state theory (HQTST), but both of these approaches were found to be less accurate for the present reaction than the CVT/μOMT approximation.[47]

Several aspects of these previous theoretical studies are important to note. The first is that the MCTDH results were obtained within the J-shifting approximation.[47] The accuracy of this approximation has never been assessed for the present reaction, but its application to other reactions suggests that the total error in the MCTDH rate coefficients in Table II should not exceed 20%, even when the other sources of error in the calculations are taken into account.[47] Since this 20% upper bound on the error in the MCTDH results is significantly less than the difference between these results and all of the other results in Table II, the MCTDH results can be regarded as an accurate benchmark against which to assess the accuracy of the other methods in the table.

We should also note that the QI results in Table II were obtained using a modified QI approach that differs from the original version of the theory in that it is recalibrated to give the correct rate coefficient in the high temperature limit.[15,46,62] This recalibration leads to better agreement with the accurate MCTDH results than the original version of the QI model. The CVT/μOMT method involves a variety of different assumptions and approximations, including a classical treatment of rotational motion and a separable harmonic oscillator treatment of vibrations.[43] These approximations are not present in either the QI model or the RPMD theory, both of which treat all degrees of freedom on an equal footing via an imaginary time path integral formulation.

To facilitate the discussion of the results in Table II we have plotted them in two different ways in Figs. 3 and 4. The first of these figures presents all of the results in the table
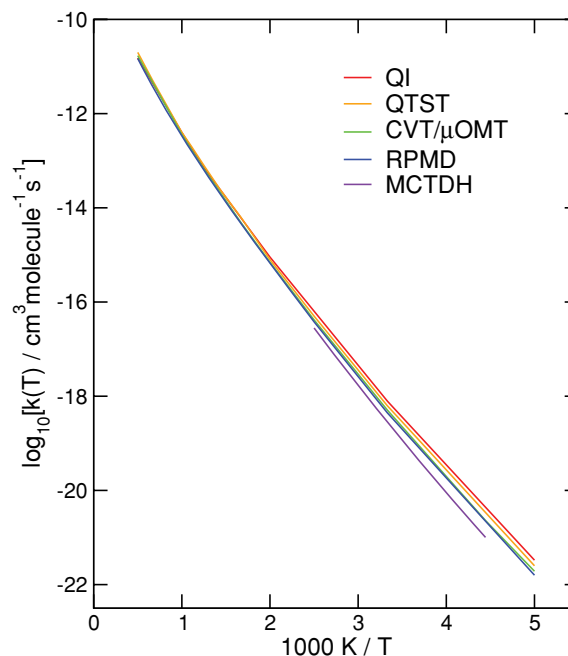

FIG. 3. Arrhenius plot of various approximate quantum mechanical rate coefficients for the H + CH₄ reaction on the PJEG potential energy surface in the temperature range from 200 to 2000 K. The results of the more accurate MCTDH calculations of Andersson *et al.*[47] are shown for comparison in the temperature range in which they are available (from 225 to 400 K).

except the classical rate coefficients (which are too small to include without extending the range of the ordinate) on an Arrhenius plot, and the second presents the percentage deviations of the approximate quantum mechanical (QI, QTST, CVT/μOMT, and RPMD) rate coefficients from the more accurate MCTDH results as a function of temperature in the range where the latter are available (from 225 to 400 K).
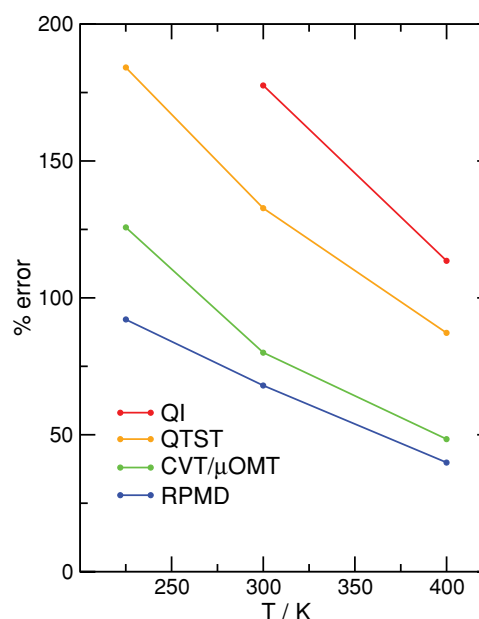

FIG. 4. Percentage deviations of the QI, QTST, CVT/μOMT, and RPMD rate coefficients for the H + CH₄ reaction from the more accurate MCTDH results in the temperature range from 225 to 400 K.

The Arrhenius plot in Fig. 3 shows that the four approximate methods give fairly similar rate coefficients which agree well in the high temperature limit but begin to spread out below around 500 K. In spite of the spread, all four approximate rate coefficients are well within an order of magnitude of the MCTDH result in the deep tunneling regime below 300 K, where the classical rate coefficient is too small by 3 orders of magnitude (see Table II). This is shown more clearly in Fig. 4, which plots the discrepancies between the various approximate rate coefficients and the more accurate MCTDH results. Clearly, of the four approximate methods we have considered, the QI model is the least accurate for this reaction, followed by the centroid density version of QTST and the CVT/μOMT approximation, respectively. The RPMD calculation gives the closest approximation to the MCTDH result throughout its available temperature range and is within a factor of 2 of this result even at 225 K. This is comparable to the accuracy of the RPMD approximation for the simpler atom–diatom reactions we considered previously.[24]

The aspect of Fig. 4 that is perhaps the most surprising is the relatively poor performance of the QI model. This is certainly one of the most sophisticated implementations of quantum transition state theory and it is often considered to be one of the most accurate. Indeed several applications of the QI model to the Eckart barrier[15,16] and atom–diatom chemical reactions in the gas phase[15,62] have shown that it provides excellent agreement with exact quantum mechanical results, significantly better than those obtained using either RPMD or the centroid density version of QTST. However this is clearly not the case for the present reaction. Presumably, this is because the sensitivity of the QI rate coefficient to the choice of reaction coordinate (and hence, after variational optimization, to the choice of the two QI dividing surfaces) becomes more of an issue as the dimensionality of the reaction increases. In fact the QI rate is less accurate than the simple centroid density QTST rate for the present reaction when it is implemented with the reaction coordinate we have used in the present study (which is the same as that used in the QI calculations reported in Ref. 46). The RPMD rate, on the other hand, is entirely independent of the choice of the reaction coordinate,[18,25] a feature that is not shared by any of the other approximate quantum mechanical methods considered in Fig. 4. This is without a doubt the single most important feature of RPMD rate theory.

IV. CONCLUDING REMARKS

In this paper, we have extended the RPMD methodology we developed in our previous paper[24] to the case of a general (polyatomic) bimolecular chemical reaction in the gas phase, and applied the resulting theory to the H + CH$_4$ reaction on a potential energy surface for which a variety of other approximate quantum mechanical rate coefficients are available for comparison.[43,46,47] We have found by comparison with accurate MCTDH benchmark results[47] that the RPMD rate is more accurate than all of these other approximate quantum mechanical rates at temperatures between 225 and 400 K (see Fig. 4). This is important because, while the MCTDH method can be used to provide benchmark results for reactions such

as H + CH$_4$, it rapidly runs out of steam for reactions with more degrees of freedom, whereas RPMD can be (and indeed has already been)[22] used to estimate the rates of considerably more complex reactions.

The comparative success of the present RPMD calculations is almost certainly owing to the independence of the RPMD rate on the choice of the transition state dividing surface.[18,25] All of the other approximate methods we have considered in Fig. 4 give a rate that is exponentially sensitive to the choice of dividing surface. For low dimensional reactions in which it is comparatively easy to construct a good dividing surface, the QI model has generally been found to be more accurate than RPMD.[15,16,62] However, as the dimensionality of the reaction increases, so does the dimensionality of the dividing surface, and even the best possible dividing surface along a well-chosen reaction coordinate becomes increasingly less likely to be optimum. The fact that the RPMD rate is independent of the dividing surface therefore becomes more of an advantage as the dimensionality of the reaction increases, as the present results already demonstrate for a reaction with as few as 6 atoms.

[1]S. C. Althorpe and D. C. Clary, Annu. Rev. Phys. Chem. **54**, 493 (2003).
[2]D. G. Truhlar and B. C. Garrett, Acc. Chem. Res. **13**, 440 (1980).
[3]D. G. Truhlar and B. C. Garrett, Annu. Rev. Phys. Chem. **35**, 159 (1984).
[4]M. J. Gillan, Phys. Rev. Lett. **58**, 563 (1987).
[5]M. J. Gillan, J. Phys. C **20**, 3621 (1987).
[6]G. A. Voth, D. Chandler, and W. H. Miller, J. Chem. Phys. **91**, 7749 (1989).
[7]A. Warshel and Z. T. Chu, J. Chem. Phys. **93**, 4003 (1990).
[8]J.-K. Hwang, Z. T. Chu, A. Yadav, and A. Warshel, J. Phys. Chem. **95**, 8445 (1991).
[9]J.-K. Hwang and A. Warshel, J. Phys. Chem. **97**, 10053 (1993).
[10]J. Cao and G. A. Voth, J. Chem. Phys. **100**, 5106 (1994).
[11]N. F. Hansen and H. C. Andersen, J. Chem. Phys. **101**, 6032 (1994).
[12]N. F. Hansen and H. C. Andersen, J. Phys. Chem. **100**, 1137 (1994).
[13]D. G. Truhlar, B. C. Garrett, and S. J. Klippenstein, J. Phys. Chem. **100**, 12771 (1996).
[14]E. Geva, Q. Shi, and G. A. Voth, J. Chem. Phys. **115**, 9209 (2001).
[15]W. H. Miller, Y. Zhao, M. Ceotto, and S. Yang, J. Chem. Phys. **119**, 1329 (2003).
[16]C. Venkataraman and W. H. Miller, J. Phys. Chem. A **108**, 3035 (2004).
[17]I. R. Craig and D. E. Manolopoulos, J. Chem. Phys. **122**, 084106 (2005).
[18]I. R. Craig and D. E. Manolopoulos, J. Chem. Phys. **123**, 034102 (2005).
[19]B. J. Braams and D. E. Manolopoulos, J. Chem. Phys. **125**, 124105 (2006).
[20]I. R. Craig and D. E. Manolopoulos, J. Chem. Phys. **121**, 3368 (2004).
[21]D. Chandler and P. G. Wolynes, J. Chem. Phys. **74**, 4078 (1981).
[22]R. Collepardo-Guevara, I. R. Craig, and D. E. Manolopoulos, J. Chem. Phys. **128**, 144502 (2008).
[23]T. E. Markland, S. Habershon, and D. E. Manolopoulos, J. Chem. Phys. **128**, 194506 (2008).
[24]R. Collepardo-Guevara, Yu. V. Suleimanov, and D. E. Manolopoulos, J. Chem. Phys. **130**, 174713 (2009); *ibid.* **133**, 049902 (2010).
[25]J. O. Richardson and S. C. Althorpe, J. Chem. Phys. **131**, 214106 (2009).
[26]C. G. Callan and S. Coleman, Phys. Rev. D **16**, 1762 (1977).
[27]G. Mills, G. K. Schenter, D. E. Makarov, and H. Jónsson, Chem. Phys. Lett. **278**, 91 (1997).

[28]W. H. Miller, J. Chem. Phys. **62**, 1899 (1975).

[29]C. H. Bennett, in *Algorithms for Chemical Computations*, ACS Symposium Series Vol. 46, edited by R. E. Christofferson (American Chemical Society, Washington, DC, 1977), p. 63.

[30]D. Chandler, J. Chem. Phys. **68**, 2959 (1978).

[31]G. M. Torrie and J. P. Valleau, Chem. Phys. Lett. **28**, 578 (1974).

[32]G. M. Torrie and J. P. Valleau, J. Comput. Phys. **23**, 187 (1977).

[33]D. Frenkel and B. Smit, *Understanding Molecular Simulation* (Academic, New York, 2002), Chaps. 15 and 16.

[34]D. Chandler, *An Introduction to Modern Statistical Mechanics* (Oxford University Press, New York, 1987).

[35]W. K. den Otter, W. J. Briels, J. Chem. Phys. **109**, 4139 (1998).

[36]J. Schlitter and M. Klähn, J. Chem. Phys. **118**, 2057 (2003).

[37]M. Sprik and G. Coccotti, J. Chem. Phys. **109**, 7737 (1998).

[38]J. Warnatz, in *Combustion Chemistry*, edited by W. C. Gardiner (Springer-Verlag, New York, 1984), p. 197.

[39]J. Pu, J. C. Corchado, and D. G. Truhlar, J. Chem. Phys. **115**, 6266 (2001).

[40]J. Pu and D. G. Truhlar, J. Chem. Phys. **116**, 1468 (2001).

[41]J. Pu and D. G. Truhlar, J. Chem. Phys. **117**, 1479 (2002).

[42]J. Pu and D. G. Truhlar, J. Chem. Phys. **117**, 10675 (2002).

[43]J. Espinosa-García, J. Chem. Phys. **116**, 10664 (2002).

[44]J. Espinosa-García, G. Nyman, and J. C. Corchado, J. Chem. Phys. **130**, 184315 (2009).

[45]J. C. Corchado, J. L. Bravo, and J. Espinosa-García, J. Chem. Phys. **130**, 184314 (2009).

[46]Y. Zhao, T. Yamamoto, and W. H. Miller, J. Chem. Phys. **120**, 3100 (2004).

[47]S. Andersson, G. Nyman, A. Arnaldsson, U. Manthe, and H. Jónsson, J. Phys. Chem. A **113**, 4468 (2009).

[48]H.-G. Yu and G. Nyman, J. Chem. Phys. **111**, 3508 (1999).

[49]D. Wang and J. M. Bowman, J. Chem. Phys. **115**, 2055 (2001).

[50]J. Palma, J. Echave, and D. C. Clary, J. Phys. Chem. A **106**, 8256 (2002).

[51]M. Wang and J. Zhang, J. Chem. Phys. **117**, 3081 (2002).

[52]M. Wang, D. H. Zhang, and S.-Y. Lee, J. Chem. Phys. **117**, 9539 (2002).

[53]B. Kerkeni and D. C. Clary, J. Chem. Phys. **120**, 2308 (2004).

[54]L. Zhang, Y. Lu, S.-Y. Lee, and D. H. Zhang, J. Chem. Phys. **127**, 234313 (2007).

[55]F. Huarte-Larrañage and U. Manthe, J. Chem. Phys. **113**, 5115 (2000).

[56]F. Huarte-Larrañage and U. Manthe, J. Phys. Chem. A **105**, 2522 (2001).

[57]F. Huarte-Larrañage and U. Manthe, J. Chem. Phys. **116**, 2863 (2002).

[58]T. Wu, H.-J. Werner, and U. Manthe, Science **306**, 2227 (2004).

[59]T. Wu, H.-J. Werner, and U. Manthe, J. Chem. Phys. **124**, 164307 (2006).

[60]G. Schiffel and U. Manthe, J. Chem. Phys. **132**, 084103 (2010).

[61]W. H. Miller, J. Chem. Phys. **61**, 1823 (1974).

[62]T. Yamamoto and W. H. Miller, J. Chem. Phys. **120**, 3086 (2004).

[63]F. Huarte-Larrañage and U. Manthe, Z. Phys. Chem. **221**, 171 (2007).

[64]J. M. Bowman, D. Wang, X. Huang, F. Huarte-Larrañage, and U. Manthe, J. Chem. Phys. **114**, 9683 (2001).

[65]U. Manthe and F. Huarte-Larrañage, Chem. Phys. Lett. **349**, 321 (2001).

[66]J. Kästner and W. Thiel, J. Chem. Phys. **123**, 144104 (2005).

[67]J. Kästner and W. Thiel, J. Chem. Phys. **124**, 234106 (2006).

[68]J. Kästner, J. Chem. Phys. **131**, 034109 (2009).

[69]M. J. T. Jordan and R. G. Gilbert, J. Chem. Phys. **102**, 5669 (1995).

[70]T. Albu, J. Espinosa-García, and D. G. Truhlar, Chem. Rev. **107**, 5101 (2007).

[71]X. Zhang, B. J. Braams, and J. M. Bowman, J. Chem. Phys. **124**, 021104 (2006).

[72]Z. Xie, J. M. Bowman, and X. Zhang, J. Chem. Phys **125**, 133120 (2006).

[73]D. L. Baulch, C. J. Cobos, R. A. Cox, C. Esser, P. Frank, Th. Just, J. A. Kerr, M. J. Pilling, J. Troe, R. W. Walker, and J. Warnatz, J. Phys. Chem. Ref. Data **21**, 411 (1992).

[74]J. W. Sutherland, M.-C. Su, and J. V. Michael, Int. J. Chem. Kinet. **33**, 669 (2001).

[75]H. C. Andersen, J. Chem. Phys. **72**, 2384 (1980).

[76]M. Ceriotti, M. Parrinello, T. E. Markland, and D. E. Manolopoulos, J. Chem. Phys. **133**, 124104 (2010).

[77]H. C. Andersen, J. Comput. Phys. **52**, 24 (1983).

[78]D. E. Makarov and M. Topaler, Phys. Rev. E **52**, 178 (1995).

[79]M. Messina, G. K. Schenter, and B. C. Garrett, J. Chem. Phys. **103**, 3430 (1995).